NO_x Removal from Simulated Flue Gas by Chemical Absorption−Biological Reduction Integrated Approach in a Biofilter

SHI-HAN ZHANG, LING-LIN CAI, XU-HONG MI, JIN-LIN JIANG, AND WEI LI*

Department of Environmental Engineering, Zhejiang University (Yuquan Campus), Hangzhou 310027, China

Received January 21, 2008. Revised manuscript received March 2, 2008. Accepted March 3, 2008.

A chemical absorption−biological reduction integrated approach, which combines the advantages of both the chemical and biological technologies, is employed to achieve the removal of nitrogen monoxide (NO) from the simulated flue gas. The biological reduction of NO to nitrogen gas (N_2) and regeneration of the absorbent Fe(II)EDTA (EDTA:ethylenediaminetetraacetate) take place under thermophilic conditions (50 ± 0.5 °C). The performance of a laboratory-scale biofilter was investigated for treating NO_x gas in this study. Shock loading studies were performed to ascertain the response of the biofilter to fluctuations of inlet loading rates (0.48∼28.68 g NO m^{-3} h^{-1}). A maximum elimination capacity (18.78 g NO m^{-3} h^{-1}) was achieved at a loading rate of 28.68 g NO m^{-3} h^{-1} and maintained 5 h operation at the steady state. Additionally, the effect of certain gaseous compounds (e.g., O_2 and SO_2) on the NO removal was also investigated. A mathematical model was developed to describe the system performance. The model has been able to predict experimental results for different inlet NO concentrations. In summary, both theoretical prediction and experimental investigation confirm that biofilter can achieve high removal rate for NO in high inlet concentrations under both steady and transient states.

Introduction

Nitrogen oxides (NO_x) could contribute to serious environmental issues, e.g., acid rain and urban ozone smoke (*1*−*3*), and health risk. For example, exposure to NO_2 at concentrations of 100 ppm or greater (30 min) can result in respiratory failure or death (*4*). Typically, the majority of the NO_x contained in a combustion flue gas stream is in the form of NO. Upon released into the ambient air, NO can be oxidized to NO_2 in the process of transport and dispersion. Therefore, reducing NO_x in the flue gas is of vital importance.

Combustion gas steams typically contain different amounts of gas compositions and fluctuate in temperature depending on the postcombustion treatments and coals. Typical flue gas after the traditional FGD process in China is estimated to contain 10∼15% (v/v) CO_2, 3∼8% (v/v) O_2, 100∼600 mg m^{-3} SO_2, 100∼1100 mg m^{-3} NO_x, and N_2. The technology designed for NO_x removal should be capable of operating under these variable conditions. To date, some physicochemical approaches have been developed to remove NO_x from the flue gas. The major drawbacks of these conventional control systems are high cost and the possibility of second pollution. Therefore, the biological techniques with cheap microbial inocula may be an alterative one. But, biological techniques show low removal efficiencies at economic retention times due to the low solubility of NO in the water (*5*). Presently, a novel chemical absorption−biological reduction integrated approach, combining the advantages of chemical and biological process, has been studied (*6, 7*). In that integrated process, Fe(II)EDTA is used to improve the NO_x absorption into the scrubbing liquid, thereby enhancing the mass transfer and overcoming the limitations associated with the biological treatment processes. The main reactions in the integrated system can be expressed as the following (*8, 9*):

$$\text{Fe(II)EDTA} + \text{NO} \rightleftharpoons \text{Fe(II)EDTA−NO} \quad (1)$$

$$4\text{Fe(II)EDTA} + \text{O}_2 + 4\text{H}^+ \rightarrow 4\text{Fe(III)EDTA} + 2\text{H}_2\text{O} \quad (2)$$

$$24\text{Fe(III)EDTA} + \text{C}_6\text{H}_{12}\text{O}_6 + 24\text{OH}^- \xrightarrow{\text{microorganism}} 24\text{Fe(II)EDTA} + 18\text{H}_2\text{O} + 6\text{CO}_2 \quad (3)$$

$$12\text{Fe(II)EDTA−NO} + \text{C}_6\text{H}_{12}\text{O}_6 \xrightarrow{\text{microorganism}} 12\text{Fe(II)EDTA} + 6\text{N}_2 + 6\text{H}_2\text{O} + 6\text{CO}_2 \quad (4)$$

NO is absorbed by Fe(II)EDTA to form Fe(II)EDTA−NO and is subsequently converted into harmless N_2 by denitrifying bacteria (*9, 10*). Since only Fe(II)EDTA can absorb NO, reduction of Fe(III)EDTA (formed via oxidation by oxygen) is an important regeneration step for sustaining the adequate NO removal. Our previous studies have demonstrated that the spent scrubber solutions (e.g., Fe(II)EDTA−NO and Fe(III)EDTA) can undergo effective regeneration by two heterotrophic bacterial strains (*8, 9*). Limited information can be obtained on the reactor employed in the integrated process. A scrubber (for chemical absorption) combining with a bioreactor (for biological regeneration) was used for NO removal in the literature (*6*). The chemical absorption of NO and biological regeneration of Fe(II)EDTA taking place in the same reactor may have the advantages of easy operation and economical cost. Thus, a biofilter was chosen for NO removal in this study due to high porosity, high nutrient availability, high moisture retention capacity, and high buffering capacity to sustain microbial growth on a suitable support matrix (*11*−*13*).

The objective of this study is to demonstrate the feasibility of using a biofilter to achieve the chemical absorption−biological reduction integrated process. Shock loadings and gaseous compositions were experimented to determine the stability and response of the microbes. A kinetic model was developed to explain the system performance. The results of this investigation provide insight on the system design, configuration, and operation.

Materials and Methods

Chemicals. Disodium ethylenediaminetetraacetate (Na_2-EDTA, 99.95%), $FeCl_2 \cdot 4H_2O$ (99.5%), $FeCl_3 \cdot 6H_2O$ (99.5%), D-glucose (99.5%) were from Shanghai Chemical Reagent Co, China. NO (5% in N_2, v/v), N_2 (99.999%), O_2 (99.999%), CO_2 (99.999%), and SO_2 (0.5% in N_2, v/v) were obtained from Zhejiang Jingong Gas Co. All other chemicals were analytical

* Corresponding author phone: 86-571-87952513; fax: 86-571-87952771; e-mail: w_li @zju.edu.cn.

10.1021/es800200g CCC: $40.75
Published on Web 04/17/2008

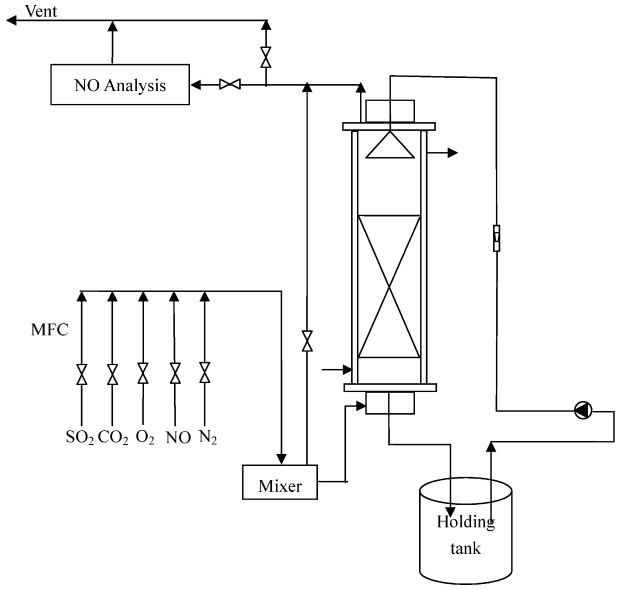

FIGURE 1. Configuration of the laboratory-scale biofilter used in the study.

grade reagents, commercially available, and used without further purification.

Microorganism Cultivation and Media Composition. The mixed culture was derived from the activated sludge of a municipal wastewater treatment plant. Two kinds of isolate, the denitrifying and Fe(III) reducing organisms, were obtained, supplementing with Fe(II)EDTA−NO and Fe(III)EDTA as the target nutrients, respectively. Based on the 16S rRNA analysis, the isolates were identified as *Pseudomonas* sp. and *Escherichia coli*, respectively (*8, 9*). The nutrient media used for continuous removal experiments have the following compositions (per liter): Glucose (1000 mg), KH_2PO_4 (300 mg), Na_2SO_3 (70 mg), $MgCl_2$ (100 mg), $CaCl_2$ (20 mg), $NaHCO_3$ (5400 mg), trace element (2 mL). The trace element for the bacteria growth includes the following components (per liter): $CoCl_2$ (240 mg), $MnCl_2 \cdot 4H_2O$ (990 mg), $CuSO_4 \cdot 5H_2O$ (250 mg), $Na_2MoO_4 \cdot 2H_2O$ (220 mg), $NiCl_2 \cdot 6H_2O$ (190 mg), H_3BO_4 (14 mg), $ZnCl_2$ (100 mg). Fe(II)EDTA and Fe(III)EDTA are prepared according to Li et al. (*8*).

Reactor Configuration. A schematic illustration of the laboratory-scale biofilter is shown in Figure 1. The biofilter column was made of acrylic cylinder with an inner diameter of 12 cm and an effective volume of 10 L. The polyhedral spheres made of polypropylene were randomly packed to provide a packed bed volume of 7.6 L. The polyhedral sphere is a commercial product with a specific surface area of 325 $m^2\ m^{-3}$. Gas sampling points were provided at the inlet and outlet of the filter bed, and the liquid sampling points were provided in a holding tank (3.5 L). The biofilter was operated in a countercurrent mode. A mixing chamber was provided before the inlet gas entered the biofilter. NO, O_2, CO_2 and SO_2 gases supplied from a commercially available standard cylinder were mixed with N_2 (99.999%) to obtain the desired concentrations when the gas flow rate was adjusted to 1 L min^{-1}. The scrubber liquor was continuously withdrawn from the holding tank and continuously pumped into the top of the biofilter at a flow rate of 40 L h^{-1}. As such, the scrubber liquor was continuously recycled. The recycled liquid provided Fe(II)EDTA (to absorb NO) and the essential nutrients necessary to sustain microbial activity. The temperature in the biofilter was controlled at 50 ± 0.5 °C with a temperature controlled water jacket to simulate the typical flue gas temperature (45∼55 °C) after the FGD process.

Biofilter Start-up. The biofilter was started up with 3 L of Fe(III)EDTA (12 mM) medium inoculated with 200 mg (DCW) L^{-1} denitrifying and Fe(III) reducing organisms, respectively. To stimulate the NO removal and regeneration of Fe(II)EDTA, the simulated flue gas contained no oxygen, but NO (315 mg m^{-3}), CO_2 (15%, v/v), and N_2 during the first 18 days of operation. To supply a certain concentration of Fe(III)EDTA to the biofilter, 300 mL fresh Fe(III)EDTA medium was added daily to the biofilter with the simultaneous withdrawal of 300 mL recycled liquor.

After a high Fe(III)EDTA reduction rate was achieved steadily, the biofilter was loaded with simulated flue gas containing O_2 (1∼5%, v/v). The inlet concentrations of O_2 were increased periodically to obtain noticeable Fe(III)EDTA reduction rate. The biofilter was operated intermittently with an average operation time of 10 h every day. Glucose was supplied to the biofilter manually as the sole electron donor and carbon source. The glucose concentration in the recycled liquid was kept above 1000 mg L^{-1} and thus glucose was present in excess of the needs by the microbes.

Experimental Procedure. After the start-up period, all the recycled liquid solution was replaced by the fresh Fe(II)EDTA (20 mM) medium. The biofilter was loaded with simulated flue gas containing NO (61∼3630 mg m^{-3}). The influence of O_2 was determined by a gradual increase of the O_2 concentration, starting with a concentration of 1∼6.5%. Additionally, the influence of SO_2 was also investigated with a gradual increase of the SO_2 concentration (from 200 to 800 mg m^{-3}). The biofilter was operated for 10 h with each change of simulated flue gas compositions, where a new steady state was achieved within 3∼5 h and maintained for the latter 5∼7 h operation.

Analytical Techniques. The inlet and outlet NO concentrations were measured with a chemiluminescent NO_x analyzer (Thermo, model 42*i*-HL). A cold trap was used to remove moisture before the gas entered the analyzer. The flux of N_2, NO, CO_2, O_2 and SO_2 supplied was controlled by the mass flow controllers (MFC) (Beijing Sevenstar Qualiflow Electronic Equipment Manufacturing Co., Ltd. model D07−12A). The Fe(II)EDTA and total iron concentrations were determined by a modified 1, 10-phenanthroline colorimetric method at 510 nm (*8*). Microscopic analyses were made using an environment scanning electron microscope (Philips, model XL30ESEM). All data shown in this paper were the mean values of duplicate or triplicate experiments.

Results and Discussions

Performance During Start-Up Period. Since the bioreduction of Fe(III)EDTA is the limiting factor in the integrated process (*8*), the Fe(III)EDTA reduction rate by microorganisms was used as a key variable to explore the performance of the biofilter during the start-up period (40 days operation). As shown in Figure 2, the Fe(III)EDTA reduction rate increased to a value of 2.12 mM h^{-1} after 18 days of operation when oxygen was absent. After that, the O_2 loading was gradually increased to evaluate how the Fe(III)EDTA reduction rate was affected. When 1% O_2 was supplied to the simulated flue gas, an obvious decrease (from 2.12 mM h^{-1} to 0.21 mM h^{-1}) of the apparent Fe(III)EDTA reduction rate was observed. The sharp decrease of the apparent Fe(III)EDTA reduction rate may be due to the easy oxidation of Fe(II)EDTA (*14*). However, the apparent reduction rate of Fe(III)EDTA gradually increased with the increase of oxygen loading from the 19th to 30th day of operation. In the last 10 days of operation, a high Fe(III)EDTA reduction rate (1.84 mM h^{-1}) was achieved steadily in presence of 5% O_2. Apparently, the microorganisms were gradually adapted to the oxygen condition and the Fe(III)EDTA reduction capacity of the biofilter was sufficient to cope with high oxygen concentrations after 40 days of cultivation. Although electrons

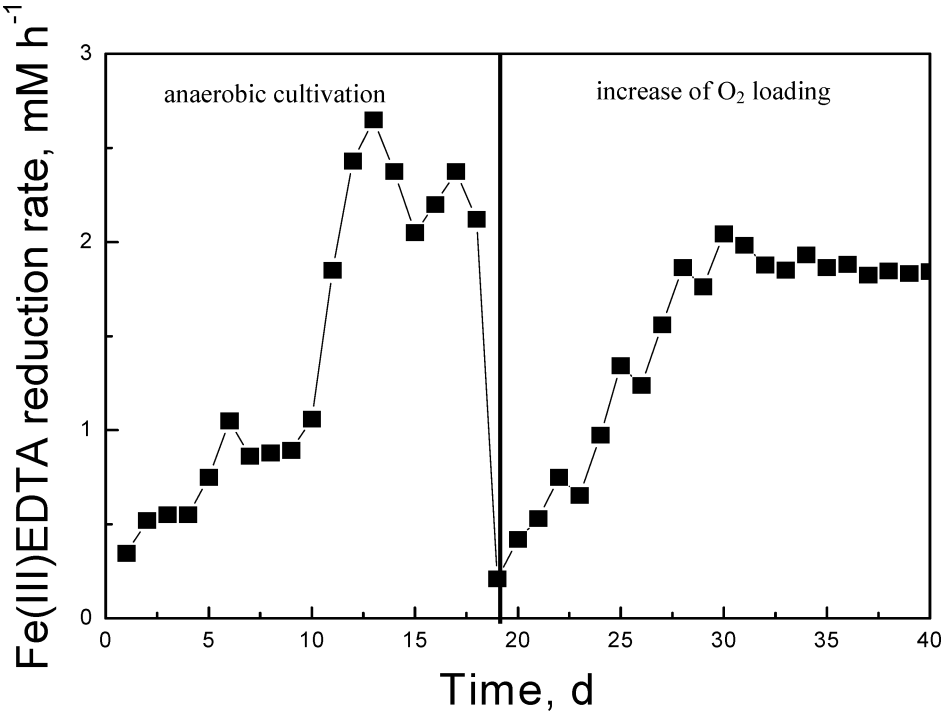

FIGURE 2. Performance of the biofilter for the Fe(III)EDTA reduction under different oxygen loadings during start-up period of operation, ([Fe(III)EDTA]$_0$ = 12 mM, oxygen concentration = 0∼5% (v/v), CO_2 concentration = 15% (v/v), NO concentration = 315 mg m^{-3}).

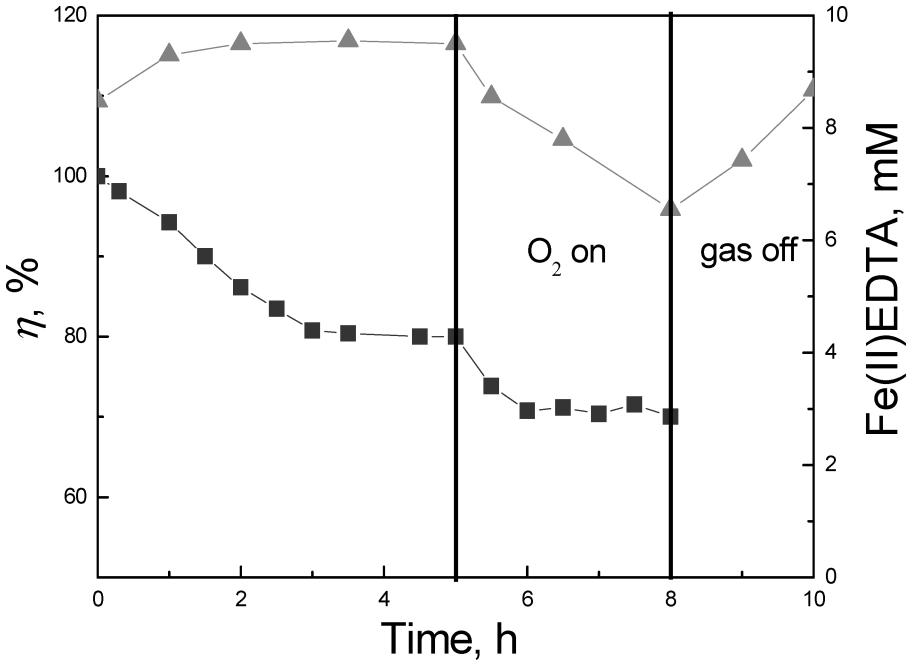

FIGURE 3. NO removal efficiency after 21 days of operation, (■) NO removal efficiency; (▲) Fe(II)EDTA ([FeEDTA]$_0$ = 12 mM, oxygen concentration = 2% (v/v), CO_2 concentration = 15% (v/v), NO concentration = 315 mg m^{-3}).

are preferentially channelled to O_2 in the electron transport chain, O_2 does not appear to inhibit Fe(III) reductase activity (*15, 16*).

When exploring the ability of NO removal, we found the NO removal efficiency (η) of the biofilter at a NO concentration of 315 mg m^{-3} during the start-up period after 21 days of operation (Figure 3) resulted in the removal of 80% of the gaseous NO in the absence of oxygen. As the O_2 concentration in the simulated flue gas was suddenly increased to 2%, Fe(II)EDTA concentration immediately decreased from 9.55 to 6.55 mM with a concurrent drop of the NO removal efficiency from 80 to 70%. The Fe(II)EDTA concentration was recovered after the gas supply was stopped.

To confirm the formation of biofilm on the polyhedral sphere surface, samples of polyhedral sphere were taken out from the middle section of the medium bed for analysis after 20 and 40 days of operation, respectively. The surface characteristic of the samples was determined by SEM. A contrast control was also performed. As shown in Figure 4, the microbial communities were established after 20 (b) and 40 (c) days of operation in comparison with the contrast one (a). These results indicate that microorganisms can grow on the filter medium. A comparison of Figure 4(b) and (c) clearly shows that the microorganism count after 40 days operation is much greater than that after 20 days operation, suggesting that formation of the biofilm was enhanced with the biofilter

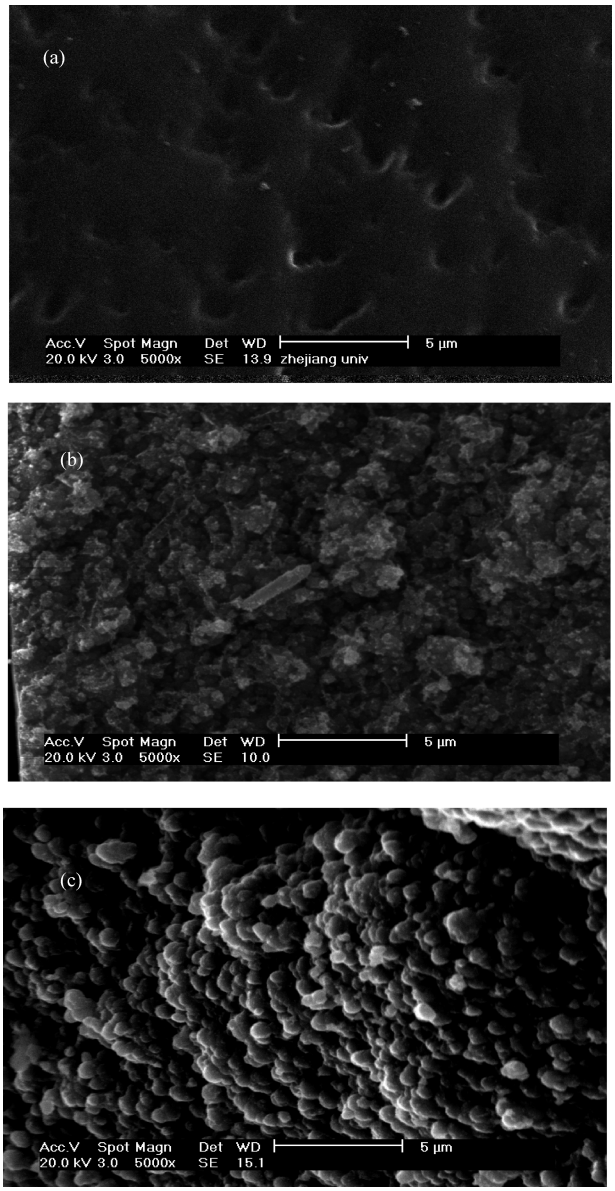

FIGURE 4. SEM Micrographs of microorganisms grown on the polyhedral spheres surfaces before (a), after 20 days (b) and 40 days (c) of cultivation.

operation. Subsequently, the increase of apparent Fe(II-I)EDTA reduction rate attributes to the abundance of microorganisms in the biofilm.

After the start-up period, continuous biofilter experiments were carried out to evaluate the removal efficiency of the biofilter to treat NO in presence of 3% oxygen. The inlet concentration of NO was increased from 61 to 1210 mg m^{-3} in periodic steps, and each step was operated till a new steady sate was achieved. A typical biofilter operation with different inlet concentration of NO is shown in Figure 5. During every step increase in the inlet NO concentration, it was observed that the biofilter took 3∼5 h to adapt to the new concentration and reached a new steady state value. The NO removal efficiency had no significant change (>70%) during the current experimental conditions. These removal profiles indicate that the biofilter well operates after the start-up period.

Effect of Shock Loading. Shock loading conditions in waste gas treatment systems are simulated by subjecting the biofilter to fluctuations in the inlet concentrations. Shock loading performance of the biofilter trial is shown in Figure

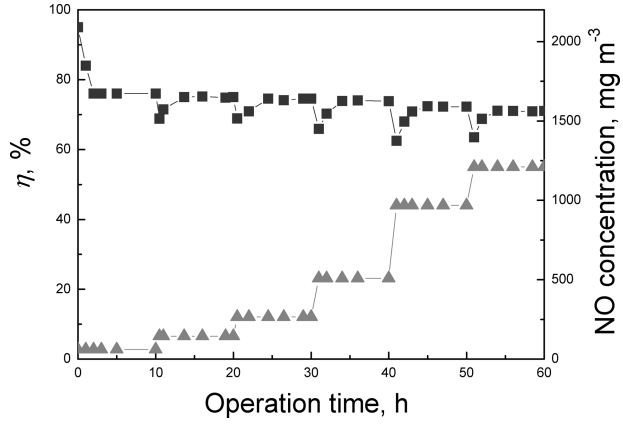

FIGURE 5. Performance of continuous biofiter operation to treat NO after the start-up period, (■) η, (▲) inlet NO concentration ([FeEDTA]$_0$ = 20 mM, CO_2 concentration = 15% (v/v), O_2 concentration = 3% (v/v)).

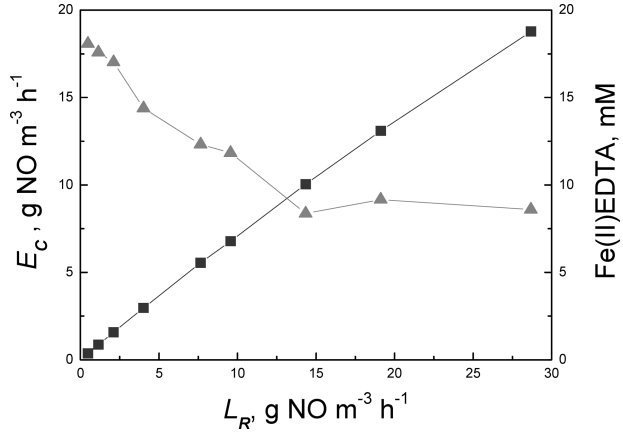

FIGURE 6. Effect of shock loading on the NO elimination capacity and Fe(II)EDTA concentration in the recycled liquor with 3% of oxygen in the simulated flue gas after the start-up period, (■) E_C; (▲) Fe(II)EDTA ([FeEDTA]$_0$ = 20 mM, Loading rates = 0.48∼ 28.68 g NO m^{-3} h^{-1}, CO_2 concentration = 15% (v/v)).

6, expressed in the form of elimination capacity (E_C) vs loading rate (L_R). E_C and L_R are defined as shown:

$$E_c = \frac{G(C_g^{in} - C_g^{out})}{V} \quad (5)$$

$$L_R = \frac{GC_g^{in}}{V} \quad (6)$$

Where, C_g^{in} and C_g^{out} are the inlet and outlet NO concentration, respectively; G is the gas flow rate and V is the volume of packed bed. The inlet loading rates were increased significantly by varying the NO concentration to values as high as 28.68 g NO m^{-3} h^{-1}. During this increase in loading rates, the NO elimination capacity increased correspondingly. A new steady state was achieved with the help of microorganisms which allowed the NO elimination capacity to be maintained after 3∼5 h operation at each loading rate. As L_R varied between 0.48 g NO m^{-3} h^{-1} and 28.68 g NO m^{-3} h^{-1}, E_C ranged from 0.36 g NO m^{-3} h^{-1} to 18.78 g NO m^{-3} h^{-1} at the steady state. Meanwhile, the concentration of Fe(II)EDTA decreased from 18.08 to 8.5 mM. Correspondingly, there was a noticeable decrease in the removal efficiency values from 76% to approximately 65.5% (data not shown).

As reported previously, the reaction of NO and O_2 could occur in the liquid phase as follows:

$$4NO + O_2 + 2H_2O \rightarrow 4NO_2^- + H^+ \quad (7)$$

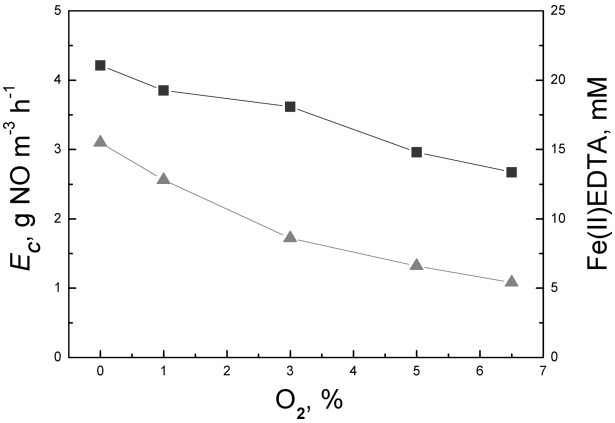

FIGURE 7. Effect of O_2 concentration on the NO elimination capacity and Fe(II)EDTA concentration in the recycled liquor after the start-up period at a loading rat of 4.97 g NO m^{-3} h^{-1}, (■) E_C; (▲) Fe(II)EDTA ([FeEDTA]$_0$ = 20 mM, O_2 concentration = 0∼6.5% (v/v), CO_2 concentration = 15% (v/v)).

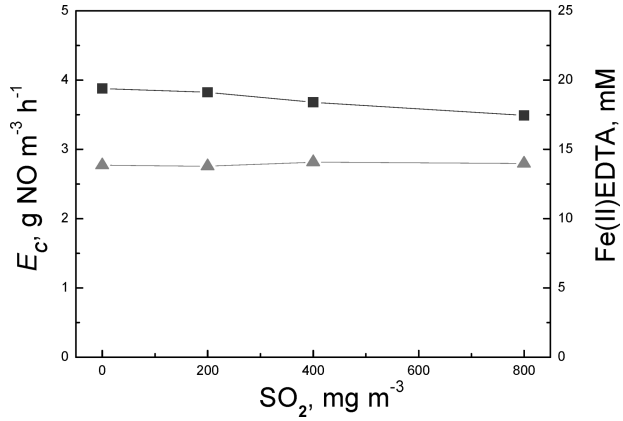

FIGURE 8. Effect of SO_2 concentration on the NO elimination capacity and Fe(II)EDTA concentration in the recycled liquor at a loading rate of 4.97 g NO m^{-3} h^{-1}, (■) E_C; (▲) Fe(II)EDTA ([FeEDTA]$_0$ = 20 mM, SO_2 concentration = 0∼800 mg m^{-3}, O_2 concentration = 1% (v/v), CO_2 concentration = 15% (v/v)).

Based on the kinetic analysis, the reaction is second-order for NO and first-order for O_2 (*17*). With the increase of inlet NO concentration, the chemical oxidization of NO into NO_2^- was promoted. An excess of nitrite would enhance the decomposition of Fe(II)EDTA−NO complexes to Fe(III)EDTA (*18*). Moreover, the oxidation of Fe(II)EDTA is accelerated by the following chemical reaction with nitrite (*19*):

$$2\text{Fe(II)EDTA} + NO_2^- + 2H^+ \rightarrow \text{Fe(III)EDTA} + \text{Fe(II)EDTA}-\text{NO} + H_2O \quad (8)$$

Additionally, Fe(II)EDTA−NO may be accumulated in the liquid phase with the increase of the NO inlet concentration. The inhibition of Fe(II)EDTA−NO on the Fe(III)EDTA reduction was reported previously (*8*). Thus, the corresponding decrease of Fe(II)EDTA concentration and NO removal efficiency were obtained.

Moreover, the experimental investigation indicates the system has the potential to remove NO at high loading conditions. However, as the loading rate was up to 14.34 g NO m^{-3} h^{-1}, the Fe(II)EDTA concentration did not decrease with the further increase of the NO loading rate. This observation could be due to the increase of Fe(III)EDTA reduction rate balanced by the Fe(II)EDTA oxidation rate increase.

Effect of Oxygen Concentration. Various chemical components present in the flue gas can interfere with the integrated process and give rise to undesired side reactions with the iron chelate. One of these components is molecular oxygen, which is typically present in the flue gas. Figure 7 shows the effect of oxygen on NO elimination capacity at a loading rate of 4.97 g NO m^{-3} h^{-1}. The NO elimination capacity gradually decreased from 4.21 g NO m^{-3} h^{-1} to 2.67 g NO m^{-3} h^{-1} with the increase of the O_2 concentration from 0 to 6.5%, along with the decrease of Fe(II)EDTA concentration from 15.5 to 5.4 mM. The easy oxidation of Fe(II)EDTA by the oxygen has been proved (*14*). Fe(III)EDTA, the oxidation product of Fe(II)EDTA, that is not capable of binding with NO and inhibits the Fe(II)EDTA−NO reduction rate (*9*), results in the decrease of the NO elimination capacity.

Effect of SO_2 Concentration. Since the flue gas usually also contains sulfurous pollutants, the possible interferences of these sulfur compounds need to be identified. Simultaneous absorption of NO and low concentration SO_2 were valuated for the potential influences of SO_2. As shown in Figure 8, with the increase of SO_2 (200∼800 mg m^{-3}), a slight decrease of NO E_C (3.82∼3.49 g NO m^{-3} h^{-1}) was observed at a loading rate of 4.97 g NO m^{-3} h^{-1}, in comparison with 3.88 g NO m^{-3} h^{-1} in absence of SO_2. However, the SO_2 had no influence on the Fe(II)EDTA concentration in the medium. The decrease of NO E_C may be due to the SO_2 influence on Fe(II)EDTA−NO biological reduction. To our best knowledge, sulfite ions, present from dissolved sulfur dioxide in this study, have been shown to be inhibitory to denitrifying bacteria (*20*). Product of the biological reduction of sulfite (sulfide) might have been present in the vials under anaerobic condition. Sulfide would result in a partial inhibition of NO reduction and be a strong inhibition of N_2O reduction (*21*).

Mathematical Model for NO Removal in Biofilter. In this study, the removal of NO in the biofilter is described by a dynamic model based on the overall mass balance. The following major assumptions were made in developing the mathematical model to describe the NO removal in the biofilter:

(1) Plug flow is assumed for the bulk gas and bulk liquid.

(2) Axial dispersion and diffusion of NO in the gas stream are negligible.

(3) Fe(II)EDTA can enhance the solubility of NO in the liquid phase but does not influence NO reduction characterization in the Biofilm.

(4) The liquid-phase NO concentration is related to the gas-phase NO concentration according to $C_L = EC_g/H$, where H is Henry's constant of NO and E is the enhanced factor of absorption capacity due to the chemical absorption.

(5) The reduction of NO in the Biofilm occurs in the reaction-limited regime.

(6) All microorganism species distribute uniformly in the biofilm under a steady state. As such, the microorganisms are treated as one kind of biomass within the biofilm.

(7) In the biofilm, no net growth of biomass is assumed so that kinetic constants remain constant over the time considered. Michaelis−Menten type kinetics is assumed.

(8) The polyhedral spheres distribute uniformly throughout the biofilter column.

Based on the above assumptions, the overall mass balance for NO in the biofilter can be expressed as the following:

$$\frac{\partial C_L}{\partial t} = GC_g|_Z - GC_g|_{z+\Delta z} + FC_L|_{z+\Delta z} - FC_L|_Z - RA\Delta z \quad (9)$$

Where C_g is the NO concentration in the gas phase; C_L is the overall NO concentration in the liquid phase; R is the NO biological reduction rate in the biofilm per volume of packed bed; A is the cross sectional area of the biofilter; and Δz is the height of the control cell.

As quasi steady state assumed, the overall mass balance now becomes

$$0 = GC_g|_z - GC_g|_{z+\Delta z} - RA\Delta z \quad (10)$$

According to Assumption 5, specific NO reduction rate in a biofilter can be expressed as the following:

$$R = \frac{\upsilon_m C_L}{K_S + C_L} \quad (11)$$

Where υ_m is the maximum reduction rate per volume of packed bed; and K_s is the half-saturation constant.

By substituting 11 into 10 and allowing $\Delta z \rightarrow 0$, the resulting model equation of the biofilter section was obtained as

$$G\frac{dC_g}{dz} = -A\frac{\upsilon_m C_L}{K_S + C_L} \quad (12)$$

Where C_L is the NO concentration in liquid phase and can be converted to EC_g/H as discussed in assumption 4. As such, eq 12 can be rewritten as

$$G\frac{dC_g}{dz} = -A\frac{\upsilon_m C_g}{k_s' + C_g} \quad (13)$$

Where

$$k_s' = \frac{K_s H}{E}; \text{ at } z = 0,\ C_g = C_g^{in}, \text{ and } z = h,\ C_g = C_g^{out} \quad (14)$$

Integrating eq 13 gives

$$\eta C_g = k_s' \ln(1-\eta) + \frac{\upsilon_m V}{G} \quad (15)$$

Where

$$\eta = \frac{C_g - C_g}{C_g} \text{ and } V = Ah \quad (16)$$

The parameter values for the equations above were determined with one set of experiments at quasi steady-state. By fitting between the models and the experimental data, k_s' and υ_m were determined to be 6857 mg m^{-3} and 76.242 g m^{-3} h^{-1}, respectively. Another set of experiments was conducted to validate the proposed model. The predicted data for the effect of inlet NO concentration on the NO removal efficiency were compared with the experimental data as shown in Figure 9. The results show that the model predictions match the experimental data satisfactorily. The maximum and average relative deviation is 1.72 and 0.75%, respectively. As the inlet NO concentration increased, the NO removal efficiency decreased in both prediction and experimental results.

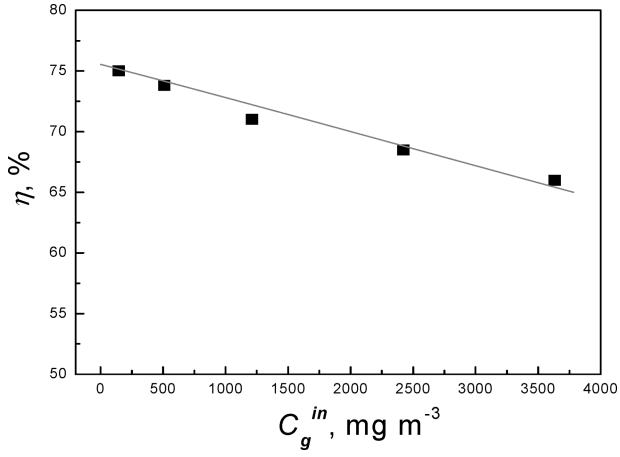

FIGURE 9. Comparison of the predicted and measured NO removal efficiency at different inlet concentration of NO, (■) measured data; (—) model predictions ([FeEDTA]$_0$ = 20 mM, CO_2 concentration = 15% (v/v), O_2 concentration = 3% (v/v)).

In summary, the findings from the study confirm the feasibility of biofilter associating with this integrated process. The increase of NO and O_2 concentrations would accelerate the oxidation rate of Fe(II)EDTA and low down the NO removal efficiency. As the NO elimination capacity decreases along with the decrease of Fe(II)EDTA concentration, the biological reduction of Fe(III)EDTA would be a key step in the integrated system as reported in the literature (*7, 10, 19*). Sulfur dioxide would inhibit the NO elimination capacity, but have no influence on the Fe(III)EDTA reduction rate. A dynamic mathematical model was constructed to explain the system performance. The modeling results confirm that the system has the potential to achieve high NO removal rates under high loading conditions.

Acknowledgments

The work was sponsored by the National High Technology Research and Development Program of China (no. 2006AA06Z345), the National Natural Science Foundation of China (no. 20676120), and the Science and Technology Project of Zhejiang Province, China (no. 2006C23064).

Appendix A

Nomenclature

E_C	NO elimination capacity (g m^{-3} h^{-1})
L_R	NO loading rate (g m^{-3} h^{-1})
C_g^{in}, C_g^{out}	Inlet and outlet NO concentrations in the gas phase (mg m^{-3})
C_L	Overall NO concentration in the liquid phase (mg m^{-3})
G	Gas flow rate (m^3 h^{-1})
V	Packed bed volume (L)
F	Liquid flow rate (m^3 h^{-1})
R	Biological NO reduction rate in the biofilm per volume of packed bed (g m^{-3} h^{-1})
A	Biofilter cross-sectional area (m^2)
h	Packed bed height (m)
υ_m	Maximum reduction rate per volume of packed bed (g m^{-3} h^{-1})
K_s	Half-saturation constant (mg m^{-3})
η	NO removal efficiency

Supporting Information Available

Additional figures and tables. This material is available free of charge via the Internet at http://pubs.acs.org.

Literature Cited

(1) Volz, A.; Kley, D. Evaluation of the montsouris series of ozone measurements made in the nineteenth century. *Nature* **1988**, *332*, 240–242.
(2) Harding, A. W.; Brown, S. D.; Thomas, K. M. Release of NO from the combustion of coal chars. *Combust. Flame* **1996**, *107*, 336–350.
(3) Solomon, S.; Portmann, R. W.; Sanders, R. W.; Daniel, J. S.; Madsen, W.; Bartram, B.; Dutton, E. G. On the role of nitrogen dioxide in the absorption of solar radiation. *J. Geophys. Res.* **1999**, *104*, 12047–12058.
(4) *Criteria for a Recommended Standard: Occupational Exposure to Oxides of Nitrogen (Nitrogen Dioxide and Nitric Oxide)*; U.S. Department of Health and Human Services, National Institute for Occupational Safety and Health: Washington, DC, 1976.
(5) Jin, Y. M.; Veiga, M. C.; Kennes, C. Review: Bioprocesses for the removal of nitrogen oxides from polluted air. *J. Chem. Technol. Biotechnol.* **2005**, *80*, 483–494.
(6) van der Maas, P.; van den Bosch, P.; Klapwijk, B.; Lens, P. NO_x removal from flue gas by an integrated physicochemical absorption and biological denitrification process. *Biotechnol. Bioeng.* **2005**, *90*, 433–441.

(7) Li, W.; Wu, C. Z.; Shi, Y. Metal chelate absorption coupled with microbial reduction for the removal of NO_x from flue gas. *J. Chem. Technol. Biotechnol.* **2006**, *81*, 306–311.
(8) Li, W.; Wu, C.-Z.; Zhang, S.-H.; Shao, K.; Shi, Y. Evaluation of microbial reduction of Fe(III)EDTA in a chemical absorption-biological reduction integrated NO_x removal system. *Environ. Sci. Technol.* **2007**, *41*, 639–644.
(9) Zhang, S.-H.; Li, W.; Wu, C.-Z.; Shi, Y. Reduction of Fe(II)EDTA—NO by a newly isolated *Pseudomonas* sp. strain DN-2 in NO_x scrubber solution. *Appl. Microbiol. Biotechnol.* **2007**, *76*, 1181–1187.
(10) van der Maas, P.; van de Sandt, T.; Klapwijk, B.; Lens, P. Biological reduction of nitric oxide in aqueous Fe(II)EDTA solutions. *Biotechnol. Prog.* **2003**, *19*, 1323–1328.
(11) Deshusses, M. A. Biological waste air treatment in biofilters. *Curr. Opin. Biotechnol.* **1997**, *8*, 335–339.
(12) Rene, E. R.; Murthy, D. V. S.; Swaminathan, T. Performance evaluation of a compost biofilter treating toluene vapours. *Proc. Biochem.* **2005**, *40*, 2771–2779.
(13) Chen, J. M.; Ma, J. F. Abiotic and biological mechanisms of nitric oxide removal from waste air in biotrickling filters. *J. Air Waste Manage. Assoc.* **2006**, *56* (1), 32–36.
(14) Gambardella, F.; Ganzeveld, I. J.; Winkelman, J. G.M.; Heeres, E J. Kinetics of the reaction of FeII (EDTA) with oxygen in aqueous solutions. *Ind. Eng. Chem. Res.* **2005**, *44*, 8190–8198.
(15) Arnold, R. G.; Hoffmann, M. R.; DiChristina, T. J.; Picardal, F. W. Regulation of dissimilatory Fe(III) reduction activity in *Shewanella putrefaciens*. *Appl. Environ. Microbiol.* **1990**, *56*, 2811–2817.
(16) Haas, J. R.; Dichristina, T. J. Effects of Fe(III) chemical speciation on dissimilatory Fe(III) reduction by *Shewanella putrefaciens*. *Environ. Sci. Technol.* **2002**, *36*, 373–380.
(17) Kharitonov, V. G.; Sundquist, A. R.; Sharma, V. S. Kinetics of nitric oxide autoxidation in aqueous solution. *J. Biol. Chem.* **1994**, *269*, 5881–5883.
(18) Zang, V.; van Eldik, R. Influence of the polyamino carboxylate chelating ligand (L) on the kinetics and mechanism of the formation of Fe^{II}(L)NO in the system Fe^{II}(L)/NO/HONO/NO_2^- in aqueous solution. *Inorg. Chem.* **1990**, *29*, 4462–4468.
(19) van der Maas, P.; Harmsen, L.; Weelink, S.; Klapwijk, B.; Lens, P. Denitrification in aqueous FeEDTA solutions. *J. Chem. Technol. Biotechnol.* **2004**, *79*, 835–841.
(20) Lee, K. H.; Sublette, K. L. Simultaneous combined microbial removal of sulfur dioxide and nitric oxid from a gas stream. *Appl. Biochem. Biotechnol.* **1991**, *28/29*, 623–634.
(21) Sørensen, J.; Tiedje, J. M.; Firestone, R. B. Inhibition by sulfide of nitric and nitrous oxide reduction by denitrifying *Pseudomonas fluorescens*. *Appl. Environ. Microbiol.* **1980**, *39*, 105–108.

ES800200G